Supplementary Information

Halogen-containing bridged carborane-tetraphenylethene compound: efficient and wide-range shifted excitation-dependent emissions

Fengjiao Li[a], Yiran Dong[a], Jinling Miao[*b], Yong Nie[*a], Yujian Zhang[*c], Tianrui Li[b], Chunyue Xu[a], Guangning Liu[b], Xuchuan Jiang[*a]

[a]Institute for Smart Materials & Engineering, University of Jinan, No. 336 Nanxinzhuang West Road, 250022 Jinan, P. R. China

[b]School of Chemistry and Chemical Engineering, University of Jinan, Shandong Provincial Key Laboratory of Fluorine Chemistry and Chemical Materials, No. 336 Nanxinzhuang West Road, 250022 Jinan, P. R. China

[c]Key Laboratory of the Ministry of Education for Advanced Catalysis Materials, Department of Chemistry, Zhejiang Normal University, No. 688 Yingbin Road, Jinhua 321004, P. R. China

E-mail: chm_niey@ujn.edu.cn, chm_miaojl@ujn.edu.cn, ism_jiangxc@ujn.edu.cn, Yujian1985@zjnu.edu.cn

Table of contents

Experimental section

General

Standard Schlenk techniques were used for the synthetic reactions under Ar. Dichloromethane was (DCM) dried with calcium hydride,, and other solvents were commercially available and used without further purification. IR spectra were recorded in the range 400-4000 cm^{-1} on a Perkin Elmer Spectrum RX I spectrometer using KBr pellets. NMR analyses were performed on a Bruker Avance III 600 MHz and 400 MHz spectrometer. ^{19}F-NMR and ^{11}B-NMR spectra were recorded in dichloromethane solutions (D_2O was added for locking) on a Bruker AVANCE III 500 spectrometer. As internal references for ^{1}H- and ^{13}C-NMR spectroscopy the signals of $CDCl_3$ were used and calculated relative to tetramethylsilane (TMS). Melting points were measured with a SGW X-4 apparatus and are not corrected. The high resolution mass spectra were measured on a Thermo Fisher Scientific LTQ FTICR-MS instrument (DART positive ion mode or ESI negative ion mode) and Waters Micromass GCT Premier (EI (70eV)). UV-Vis spectra were recorded on a UV3600 Plus spectrometer. Emission spectra were measured on Edinburgh FLS920 and FLS1000 fluorimeters, using a front-face sample configuration for solid samples. Absolute fluorescence quantum yields were obtained using an integrating sphere.

Synthesis of compound 1

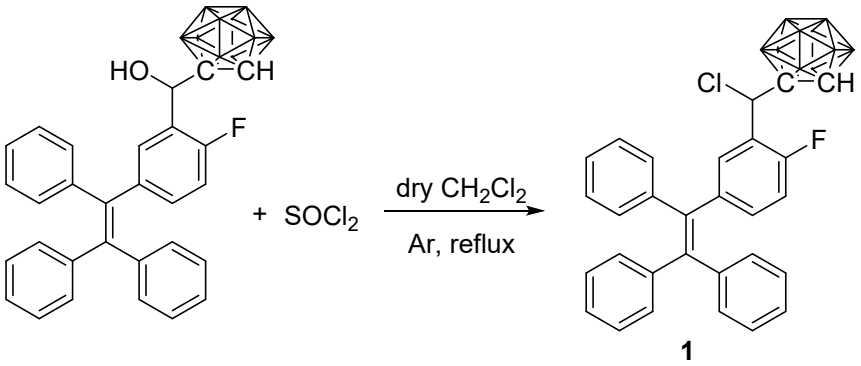

1

Under argon, the starting carboranylmethanol compound (103.7 mg, 0.2 mmol) and 5 mL of dry CH_2Cl_2 were added into a Schlenk tube and stirred, to this solution was added 0.5 mL of $SOCl_2$ (6.9 mmol) via syringe. The reaction mixture was heated at 45 ^{o}C (oil bath) for 24 h, during which time the reaction was completed as monitored by TLC. The reaction mixture was poured into a cold saturated aqueous solution of K_2CO_3 (20 mL) and separated. The water phase was extracted with CH_2Cl_2 (3 × 20 mL) and the combined organic phases were dried with anhydrous Na_2SO_4. After filtration and concentration the solution was separated by preparative TLC (eluent: EtOAc: hexane =

1:5, *V*/*V*) to give a yellow oil, which solidified after adding 2 mL of CH_2Cl_2 and cured for 24 h to afford compound **1** as a white solid.

1: 52.8 mg, yield 48.8%; *m.p.* 149.7 °C; R_f = 0.82 (EtOAc: hexane = 1:5, *V*/*V*) ; IR (KBr, ν/cm^{-1}): 3055, 2924, 2588 (BH), 1597, 1491, 1441, 1248, 847, 768, 741, 700; ^{1}H NMR (600 MHz, $CDCl_3$) δ 7.20 - 7.12 (m, 10 H, ArH), 7.04 - 7.02 (m, 5 H, ArH), 6.97 - 6.96 (m, 2 H, ArH), 6.87, 6.85 (t, *J* = 9.32 Hz, 1H, ArH), 5.76 (s, 1 H, CHCl), 3.54 (s, 1 H, $C_{cage}H$); ^{13}C NMR (151 MHz, $CDCl_3$) δ: 158.10, 156.45, 143.07, 142.97, 142.85, 142.19, 141.05, 138.76, 134.56 (d, *J* = 7.55 Hz), 132.27, 131.29, 131.17 (d, *J* = 9.06 Hz), 128.20, 127.96, 127.78, 127.26, 126.87 (d, *J* = 6.04 Hz), 123.83 (d, *J* = 12.05 Hz), 115.22, 115.08, 76.50, 61.05, 54.12; ^{11}B{^{1}H} NMR (128 MHz, CH_2Cl_2): δ -3.22 (1B), -4.43 (1B), -8.68 (1B), -9.33 (1B), -10.74 (1B), -11.73 (1B), -12.75 (2B), -14.00 (2B); ^{19}F NMR (377 MHz, CH_2Cl_2) δ: -119.46; ESI-MS *m/z*(%): calcd. for $C_{29}H_{29}B_{10}FCl$, 541.2878 [M-H]$^-$, found 541.2875.

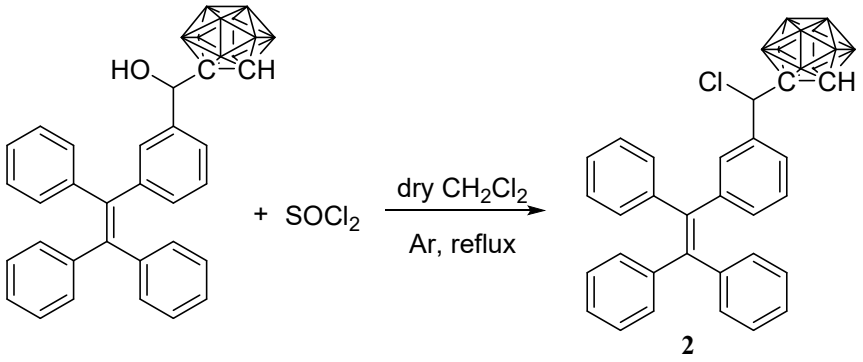

2

Under argon, the starting carboranylmethanol compound (100.9 mg, 0.2 mmol) and 5 mL of dry CH_2Cl_2 were added into a Schlenk tube and stirred, to this solution was added 0.5 mL of $SOCl_2$ (6.9 mmol) via syringe. The reaction mixture was heated at 45 °C (oil bath) for 24 h, during which time the reaction was completed as monitored by TLC. The reaction mixture was poured into a cold saturated aqueous solution of K_2CO_3 (20 mL) and separated. The water phase was extracted with CH_2Cl_2 (3 × 20 mL) and the combined organic phases were dried with anhydrous Na_2SO_4. After filtration and concentration the solution was separated by preparative TLC (eluent: EtOAc: hexane = 1:5, *V*/*V*) to give a yellow oil, which solidified after adding 2 mL of CH_2Cl_2 and cured for 24 h to afford compound **2** as a white solid.

2: 75.2 mg, yield 72.0%; *m.p.* 175.2 °C; R_f = 0.84 (EtOAc: hexane = 1:5, *V*/*V*) ; IR (KBr, ν/cm^{-1}): 3053, 2922, 2851, 2578(BH), 1597, 1489, 1441, 1096, 1020, 758, 698; ^{1}H NMR (600 MHz, $CDCl_3$) δ 7.16 (t, *J* = 7.6 Hz, 1H, ArH), 7.11 (m, 10H, ArH), 7.09 (d, *J* = 7.6 Hz, 1H, ArH), 7.04 - 7.01 (m,

5H, ArH), 6.97 (m, 2H, ArH), 5.26 (s, 1H, CHCl), 3.54 (s, 1H, $C_{cage}H$);^{13}C NMR (151 MHz, $CDCl_3$) δ 144.85, 143.20, 143.07, 143.04, 142.14, 139.60, 136.01, 132.94, 131.33, 131.24, 131.19, 130.80, 128.37, 128.05, 127.88, 127.76, 126.78, 126.76, 126.04, 62.45, 61.17; $^{11}B\{^1H\}$ NMR (128 MHz, CH_2Cl_2): δ -3.35 (1B), -4.38 (1B), -8.64 (1B), -9.32 (1B), -10.51 (1B), -11.81 (1B), -12.80 (2B), -14.01 (2B); DART-MS m/z(%): calcd. for $C_{29}H_{32}B_{10}Cl$ $[M+H]^+$, 525.3188, found 525.3162.

Table S1 Crystal data and structure refinement for **1**

Compound	**1**
Empirical formula	$C_{29}H_{30}B_{10}ClF$
Formula weight	541.08
Temperature/K	293(2)
Crystal system	monoclinic
Space group	C2/c
a/Å	14.1612(4)
b/Å	12.8676(4)
c/Å	31.9346(10)
α/°	90
β/°	98.367(3)
γ/°	90
Volume/Å^3	5757.2(3)
Z	8
ρ_{calc}g/cm^3	1.248
μ/mm^{-1}	0.159
F(000)	2240
Crystal size/mm^3	0.2×0.18×0.08
Radiation	MoKα (λ = 0.71073)
2Θ range for data collection/°	4.298 to 56.562
Index ranges	-16 ≤ h ≤ 18, -17≤ k ≤ 17, -42 ≤ l ≤ 42
Reflections collected	8724
Independent reflections	8724 [R_{int} = , R_{sigma} = 0.0296]
Data/restraints/parameters	8724/0/373
Goodness-of-fit on F^2	1.123
Final R indexes [I>=2σ (I)]	R_1 = 0.0746, wR_2 = 0.2028
Final R indexes [all data]	R_1 = 0.0823, wR_2 = 0.1816
Largest diff. peak/hole / e Å^{-3}	0.478/-0.515
CCDC deposition number	2304126

Table S2. Selected bond lengths, angles and torsion angles for **1**

bond lengths (Å)		bond angles [°]		torsion angles [°]	
C1-C2	1.394	C1-C2-C3	120.07	C1-C2-C3-C4	-1.09
C2-C3	1.398	C2-C3-C4	119.93	C6-C1-C7-C8	-48.54
C3-C4	1.380	C1-C7-C8	114.77	C1-C7-C8-C9	-48.20
C1-C7	1.499	C7-C8-C13	122.75	C8-C7-C14-C21	-6.43
C7-C8	1.498	C7-C8-C9	118.57	C26-C25-C27-Cl1	-39.60
C8-C9	1.403	C8-C7-C14	122.79	C27-C25-C24-F1	2.30
C7-C14	1.349	C25-C27-C28	114.88	Cl1-C27-C28-C29	20.89
C14-C21	1.505	C24-C25-C27	119.51		
C21-C22	1.386	C25-C27-Cl1	110.01		
C23-C24	1.383	C27-C28-C29	120.98		
C24-F1	1.355				
C25-C27	1.505				
C27-C28	1.545				
C28-C29	1.641				
C27-Cl1	1.791				

Table S3 Weak interactions in crystals of compound **1**

D–H···A	d(H···A) [Å]	d(D···A) [Å]	∠(D–H···A) [°]
B(4)-H(4A)···Cg(1)	2.642	3.645	151.17
C(29)-H(29)···Cl(1)	2.738	3.118	99.76
C(26)-H(26)···Cl(1)	2.774	3.073	99.83
C(27)-H(27)…F(1)	2.333	2.772	106.24
C(5)-H(5)···Cg(2)	2.870	3.596	135.8
C(24)-F(1)···Cg(1)	3.456	4.579	140.14
C(29)-H(29)···H(7)-B7	2.267	2.982	120.65

Cg(1)：(C8, C9, C10, C11, C12, C13), Cg(2)：(C21, C22, C23, C24, C25, C26)

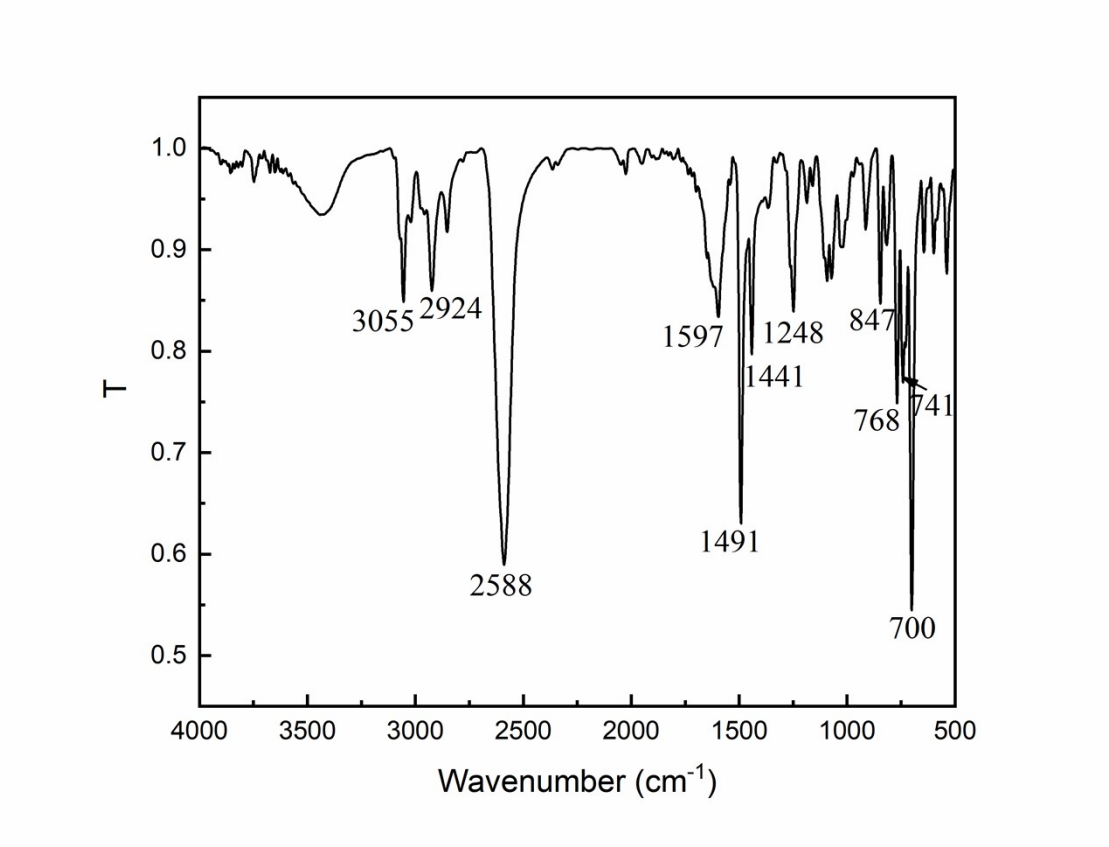

Fig. S1. FT-IR spectrum of **1** (KBr pellet)

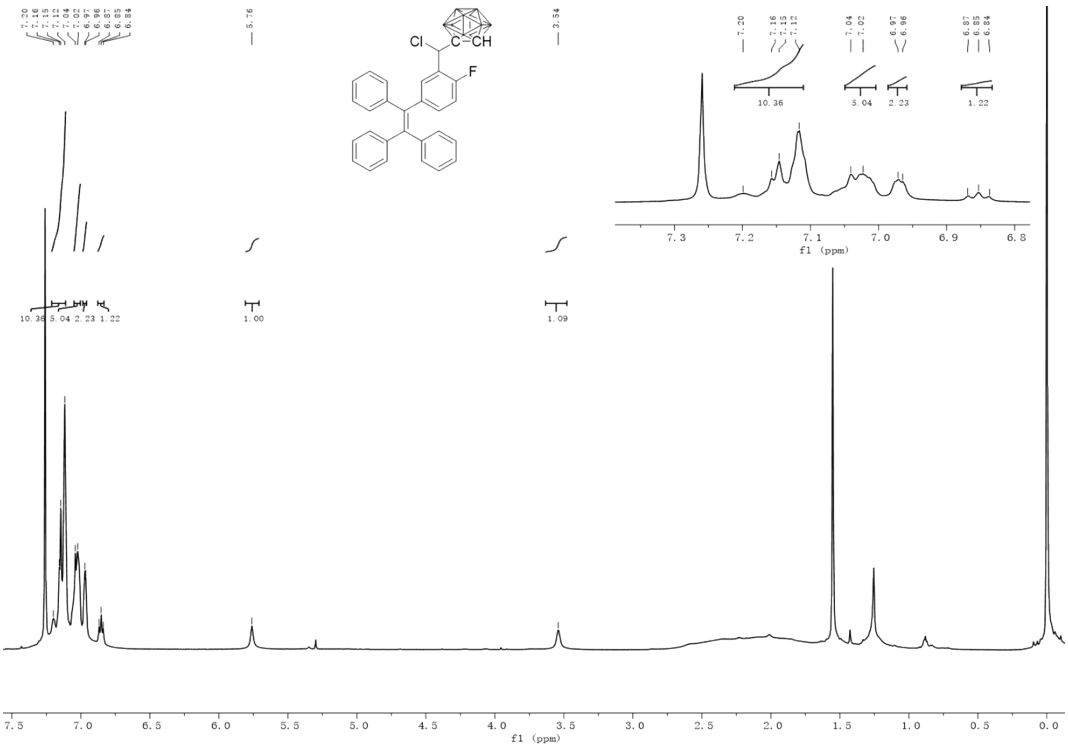

Fig. S2. ^{1}H-NMR spectrum of **1** in $CDCl_3$

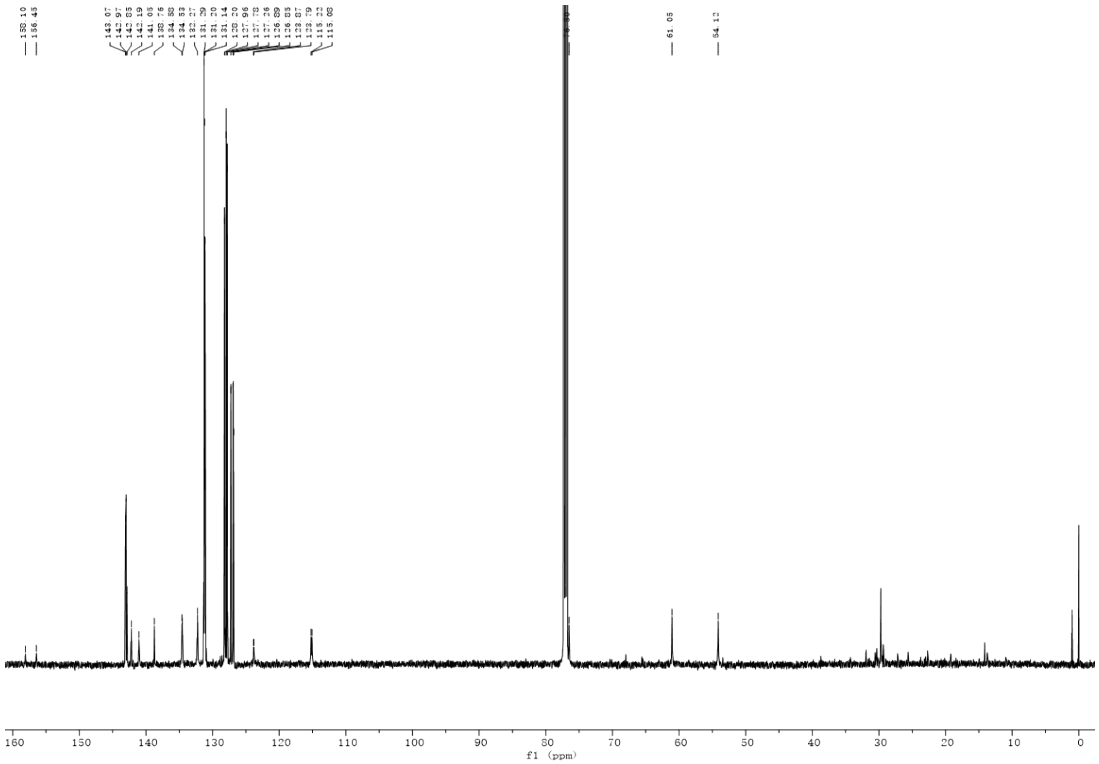

Fig. S3. ^{13}C-NMR spectrum of **1** in $CDCl_3$

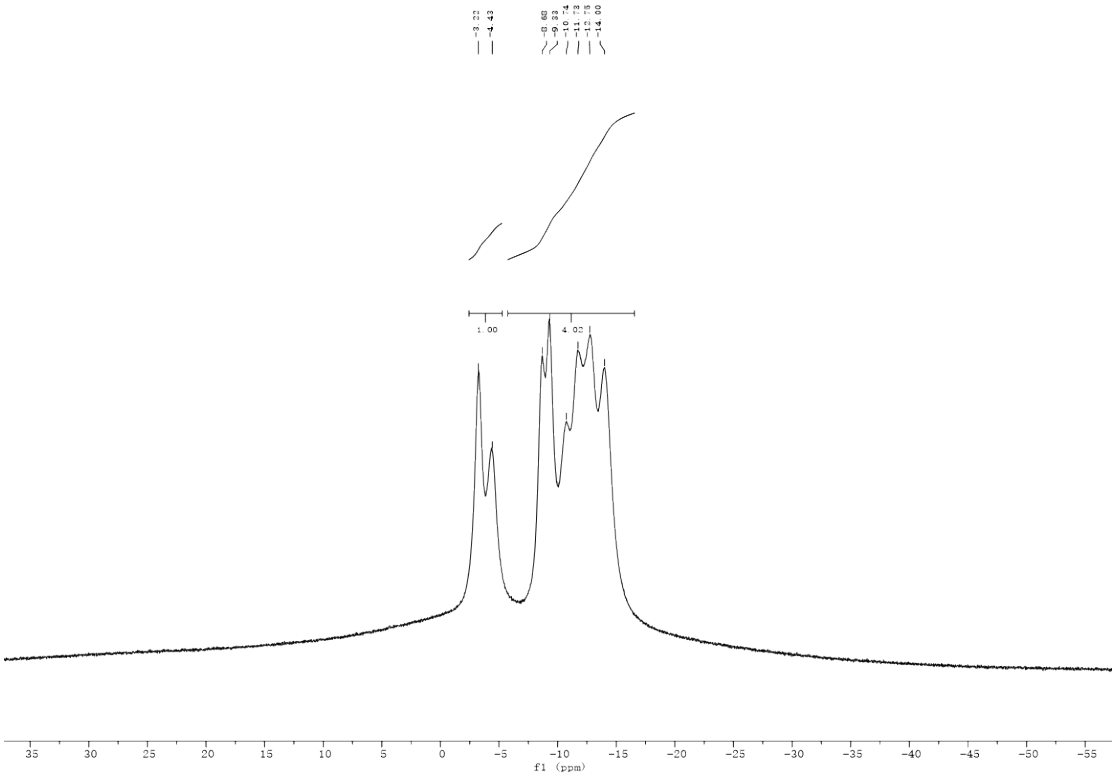

Fig. S4. $^{11}B\{^1H\}$-NMR spectrum of **1** in CH_2Cl_2

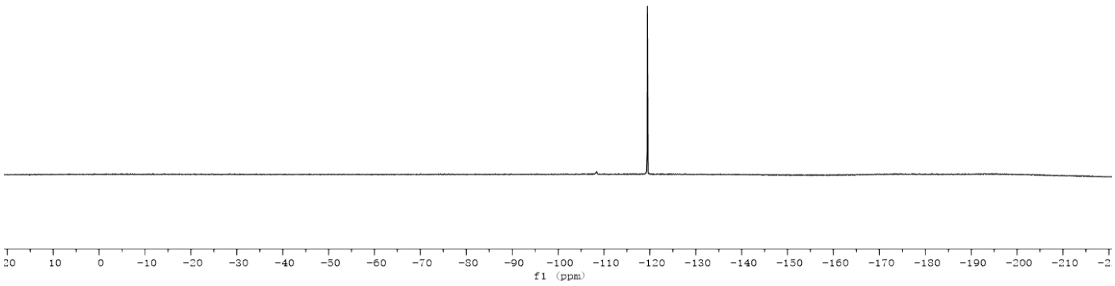

Fig. S5. ^{19}F-NMR spectrum of **1** in CH_2Cl_2

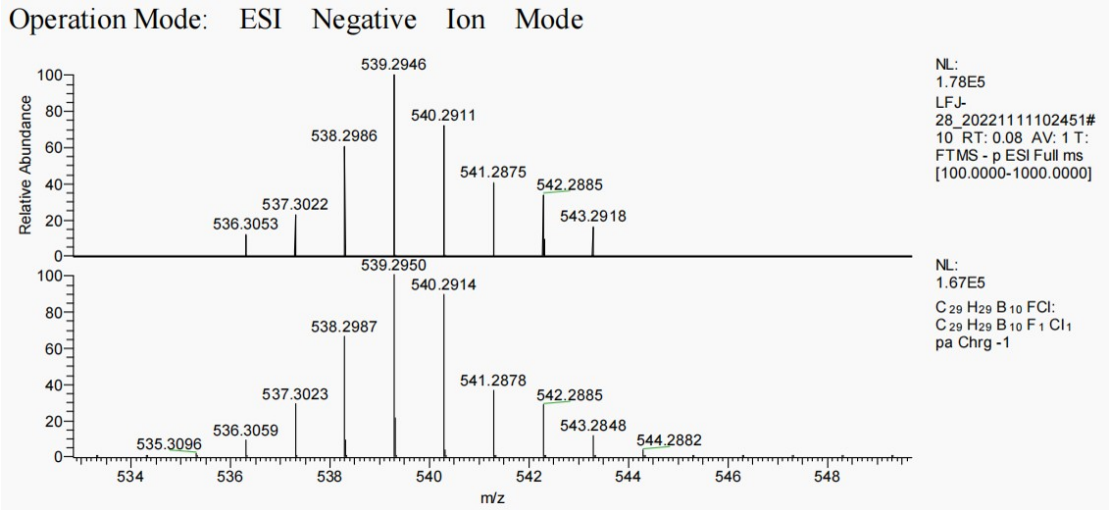

Fig. S6. High resolution mass spectrum of **1** (top: experimental, bottom: theoretical)

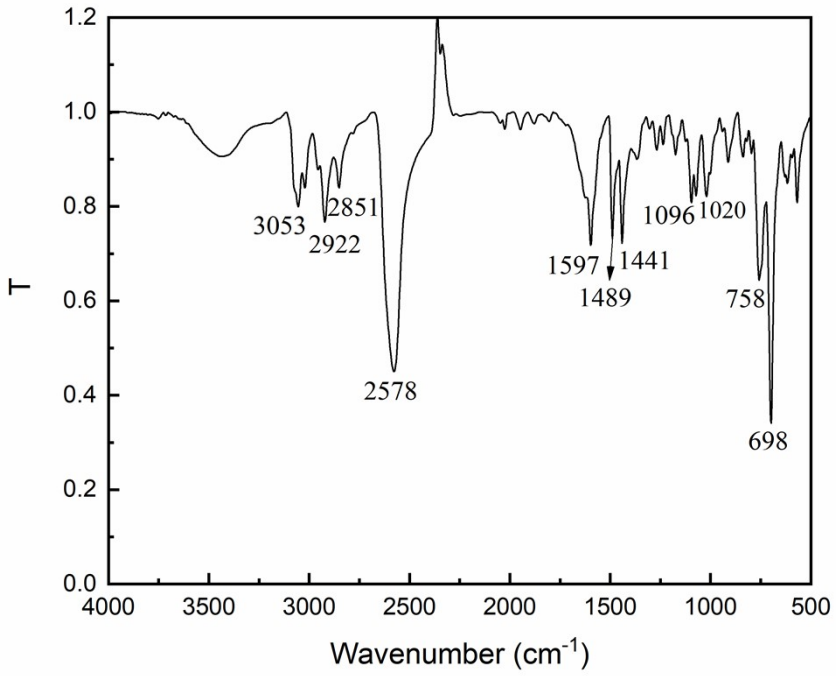

Fig. S7. FT-IR spectrum of **2** (KBr pellet)

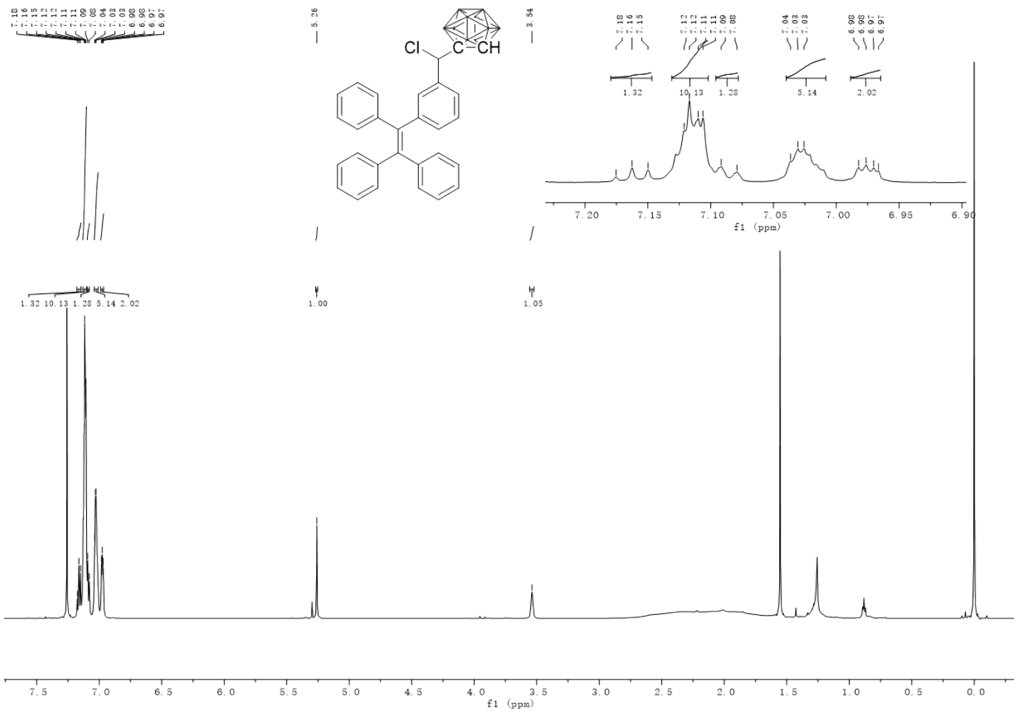

Fig. S8. ^{1}H-NMR spectrum of **2** in $CDCl_3$

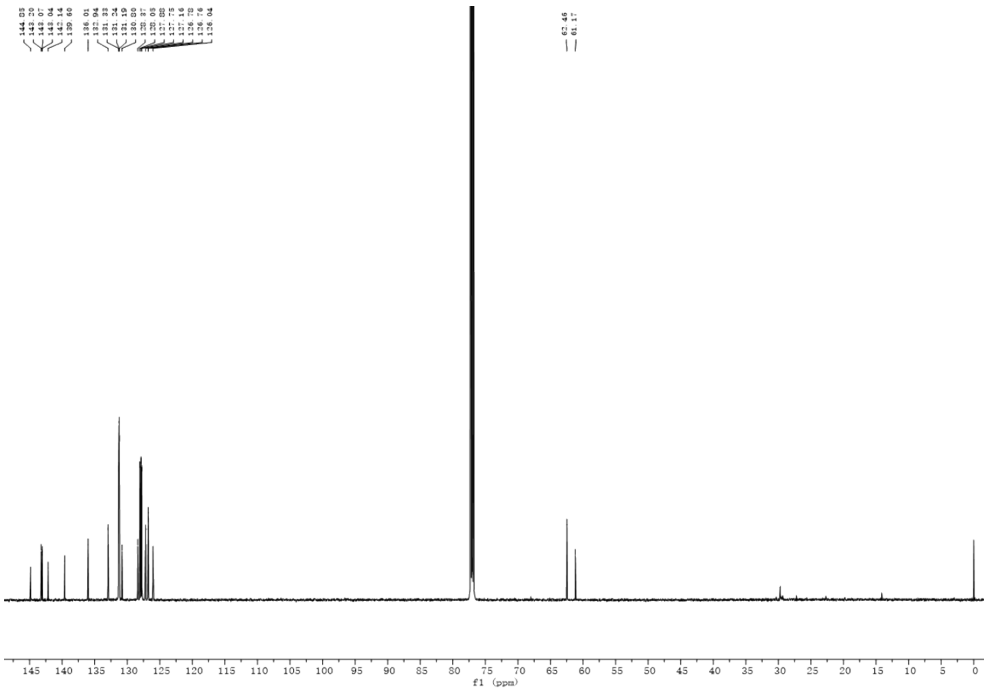

Fig. S9. ^{13}C-NMR spectrum of **2** in $CDCl_3$

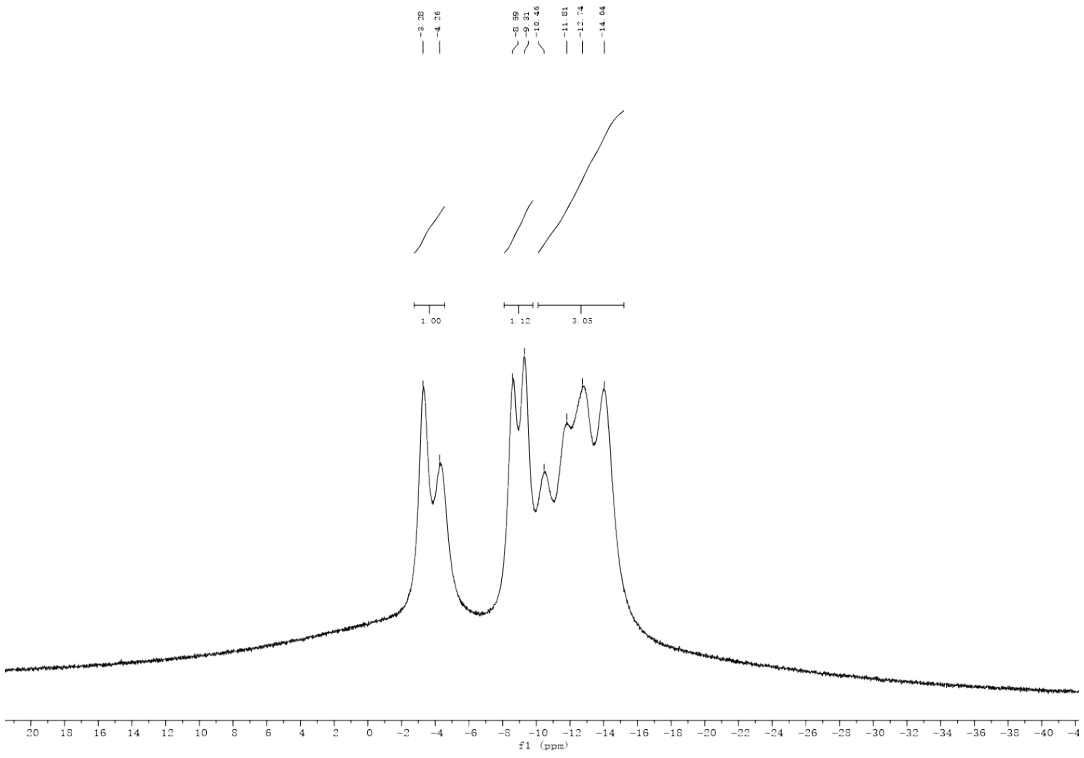

Fig. S10. $^{11}B\{^1H\}$-NMR spectrum of **2** in CH_2Cl_2

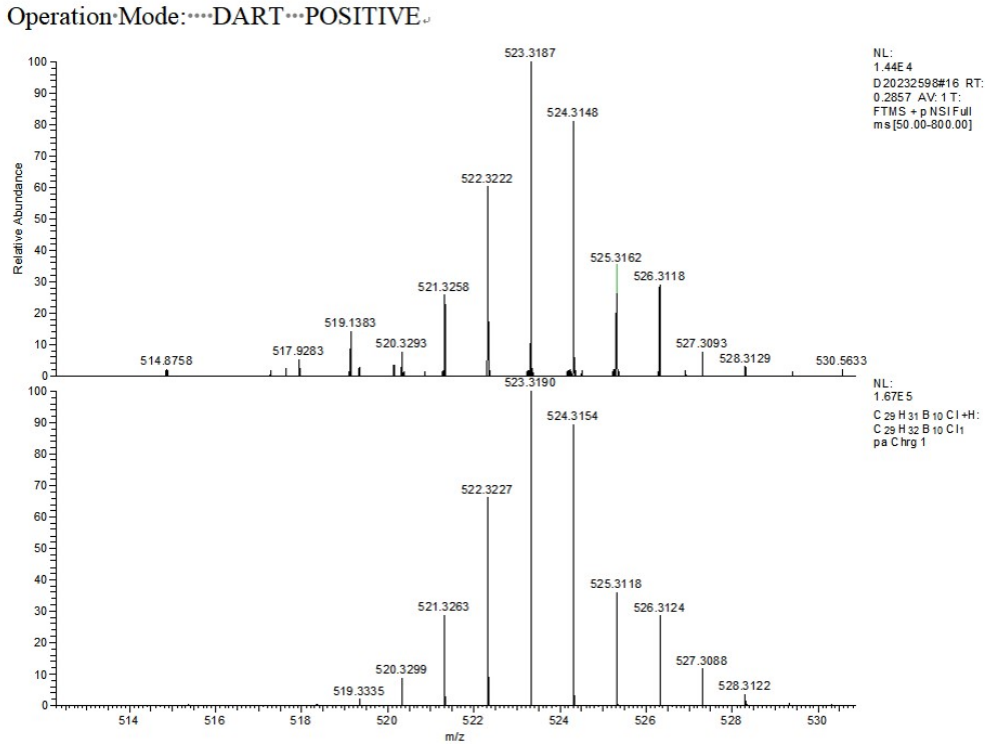

Figure S11 High resolution mass spectrum of **2** (top: experimental, bottom: theoretical)

Reference for the Gaussian package for the DFT calculations:

M. J. Frisch, G. W. Trucks, H. B. Schlegel, G. E. Scuseria, M. A. Robb, J. R. Cheeseman, G. Scalmani, V. Barone, B. Mennucci, G. A. Petersson, H. Nakatsuji, M. Caricato, X. Li, H. P. Hratchian, A. F. Izmaylov, J. Bloino, G. Zheng, J. L. Sonnenberg, M. Hada, M. Ehara, K. Toyota, R. Fukuda, J. Hasegawa, M. Ishida, T. Nakajima, Y. Honda, O. Kitao, H. Nakai, T. Vreven, J. A. Montgomery, Jr., J. E. Peralta, F. Ogliaro, M. Bearpark, J. J. Heyd, E. Brothers, K. N. Kudin, V. N. Staroverov, R. Kobayashi, J. Normand, K. Raghavachari, A. Rendell, J. C. Burant, S. S. Iyengar, J. Tomasi, M. Cossi, N. Rega, J. M. Millam, M. Klene, J. E. Knox, J. B. Cross, V. Bakken, C. Adamo, J. Jaramillo, R. Gomperts, R. E. Stratmann, O. Yazyev, A. J. Austin, R. Cammi, C. Pomelli, J. W. Ochterski, R. L. Martin, K. Morokuma, V. G. Zakrzewski, G. A. Voth, P. Salvador, J. J. Dannenberg, S. Dapprich, A. D. Daniels, O. Farkas, J. B. Foresman, J. V. Ortiz, J. Cioslowski, and D. J. Fox, Gaussian 09, Revision A.02, Gaussian, Inc., Wallingford CT, 2009.

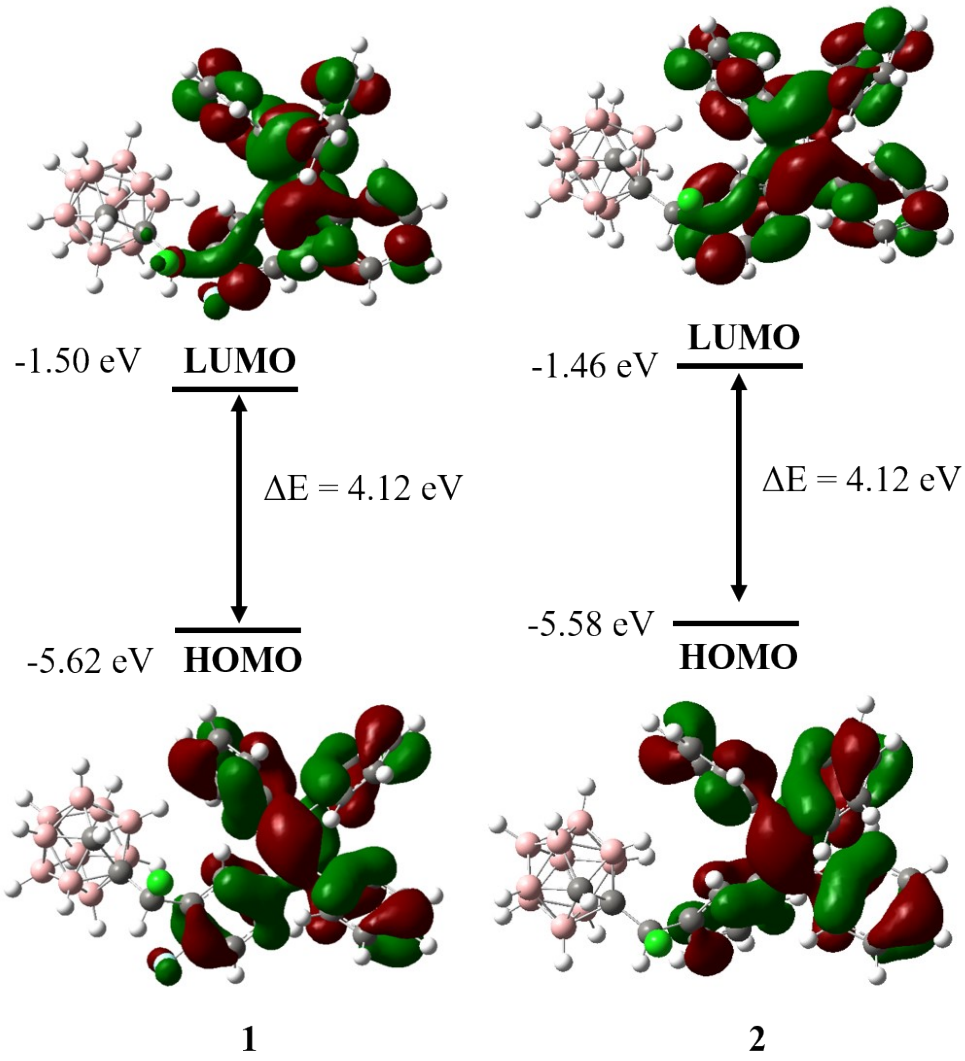

Fig. S12 Frontier orbitals and energy levels of compounds **1-2** (B3LYP/ 6-31g (d, p) level)

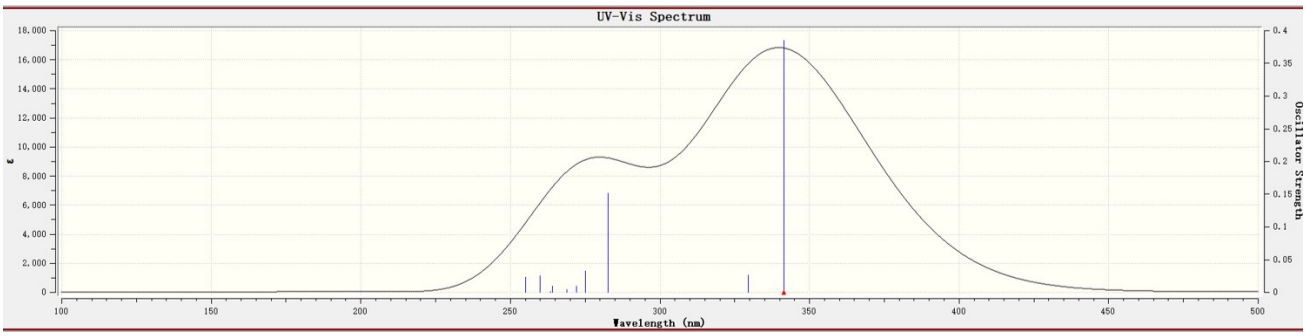

Fig. S13 Absorption spectrum of **1** in tetrahydrofuran calculated by TD-DFT method

Table S4 Excitation energy and transitions of **1** in tetrahydrofuran calculated by TD-DFT method[a]

state	E (eV)	λ (nm)	*f*	transitions
1	3.6303	341.53	0.3856	HOMO→LUMO (99.1%)
2	3.7614	329.62	0.0265	HOMO→LUMO + 1 (97.7%)
3	4.3870	282.62	0.1521	HOMO - 5→LUMO (2.8%)

				HOMO→LUMO + 2 (90.3%)
	4	4.5075	275.06	0.0325 HOMO - 1→LUMO (34.0%)
				HOMO→LUMO + 2 (4.0%)
				HOMO→LUMO + 3 (36.1%)
				HOMO→LUMO + 4 (11.1%)
				HOMO→LUMO + 5 (4.0%)
				HOMO→LUMO + 6 (2.7%)
	5	4.5552	272.18	0.0093 HOMO - 3→LUMO (2.3%)
				HOMO - 1→LUMO (42.5%)
				HOMO→LUMO + 3 (36.7%)
				HOMO→LUMO + 4 (4.3%)
				HOMO→LUMO + 5 (9.5%)
6		4.6127	268.79	0.0038 HOMO - 2→LUMO (79.2%)
				HOMO - 2→LUMO + 1 (2.2%)
				HOMO→LUMO + 4 (2.2%)
				HOMO→LUMO + 7 (2.3%)
				HOMO→LUMO + 8 (6.6%)
7		4.6955	264.05	0.0098 HOMO - 4→LUMO (5.1%)
				HOMO - 3→LUMO (9.8%)
				HOMO→LUMO + 3 (19.6%)
				HOMO→LUMO + 4 (39.8%)
				HOMO→LUMO + 5 (13.1%)
				HOMO→LUMO + 6 (7.1%)
	8	4.7059	263.47	0.0015 HOMO - 4→LUMO (5.8%)
				HOMO - 3→LUMO (46.5%)
				HOMO - 2→LUMO (1.1%)
				HOMO - 1→LUMO (3.1%)
				HOMO→LUMO + 4 (9.8%)
				HOMO→LUMO + 5 (2.9%)
				HOMO→LUMO + 6 (4.9%)
				HOMO→LUMO + 7 (16.9%)
	9	4.7684	260.01	0.0254 HOMO - 3→LUMO (9.7%)
				HOMO - 1→LUMO(13.3%)
				HOMO→LUMO + 5 (59.3%)
				HOMO→LUMO + 6 (5.4%)
	10	4.8626	254.98	0.0227 HOMO - 7→LUMO (2.8%)
				HOMO - 4→LUMO (4.8%)
				HOMO - 4→LUMO + 1 (2.3%)
				HOMO - 2 →LUMO + 1 (7.9%)
				HOMO - 1→LUMO + 1 (62.0%)
				HOMO→LUMO + 4 (4.3%)
				HOMO→LUMO + 7 (3.7%)

[a]calculated at the B3LYP/6-31G (d,p) level of theory.

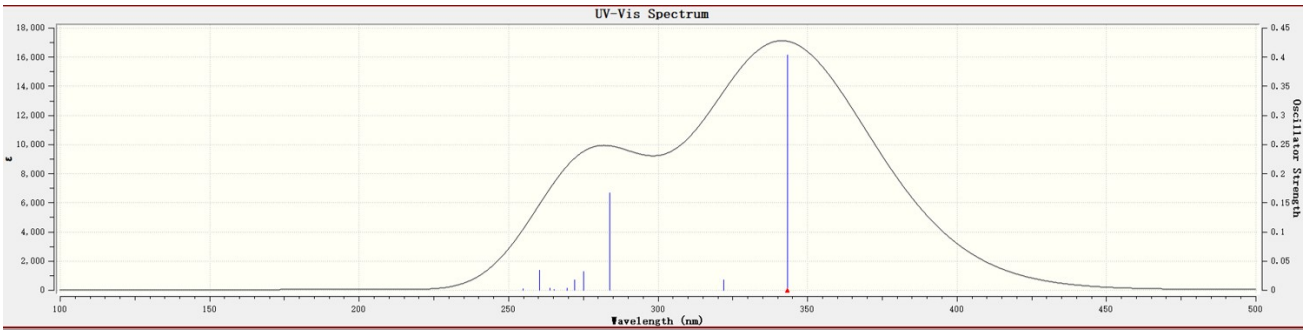

Fig. S14 Absorption spectrum of **2** in tetrahydrofuran calculated by TD-DFT method

Table S5 Excitation energy and transitions of **2** in tetrahydrofuran calculated by TD-DFT method[a]

state	E (eV)	λ (nm)	*f*	transitions
1	3.6127	343.19	0.4038	HOMO→LUMO (99.1%)
2	3.8500	322.03	0.0176	HOMO→LUMO + 1 (97.2%)
3	4.3683	283.83	0.1669	HOMO→LUMO + 2 (91.6%)
4	4.5055	275.18	0.0324	HOMO - 1→LUMO (42.9%) HOMO→LUMO + 3 (22.0%) HOMO→LUMO + 4 (17.2%) HOMO→LUMO + 5 (7.5%)
5	4.5569	272.08	0.0180	HOMO - 3→LUMO (4.4%) HOMO - 1→LUMO (29.4%) HOMO→LUMO + 3 (37.0%) HOMO→LUMO + 4 (11.5%) HOMO→LUMO + 5 (11.5%)
6	4.6013	269.45	0.0039	HOMO - 2→LUMO (79.3%) HOMO - 1→LUMO (2.8%) HOMO→LUMO + 8 (6.5%)
7	4.6747	265.22	0.0009	HOMO - 4→LUMO (3.6%) HOMO - 3→LUMO (57.2%) HOMO - 2→LUMO (5.1%) HOMO - 1→LUMO (3.3%) HOMO→LUMO + 4 (2.2%) HOMO→LUMO + 5 (6.1%) HOMO→LUMO + 6 (3.9%) HOMO→LUMO + 7 (10.9%)
8	4.7012	263.73	0.0040	HOMO - 4→LUMO (9.4%) HOMO - 3→LUMO (6.6%) HOMO - 1→LUMO (2.4%) HOMO→LUMO + 3 (28.3%) HOMO→LUMO + 4 (33.8%)

				HOMO→LUMO + 6 (11.8%)
9	4.7608	260.43	0.0349	HOMO - 3→LUMO (6.8%) HOMO - 1→LUMO (13.6%) HOMO→LUMO + 4 (2.5%) HOMO→LUMO + 5 (68.3%)
10	4.8663	254.78	0.0023	HOMO - 5→LUMO (2.8%) HOMO - 4→LUMO (32.5%) HOMO - 3→LUMO (17.4%) HOMO - 1 →LUMO + 1 (2.4%) HOMO →LUMO + 3 (4.3%) HOMO→LUMO + 4 (22.9%) HOMO→LUMO + 6 (16.3%) HOMO→LUMO + 7 (3.6%)

[a]calculated at the B3LYP/6-31G (d,p) level of theory.

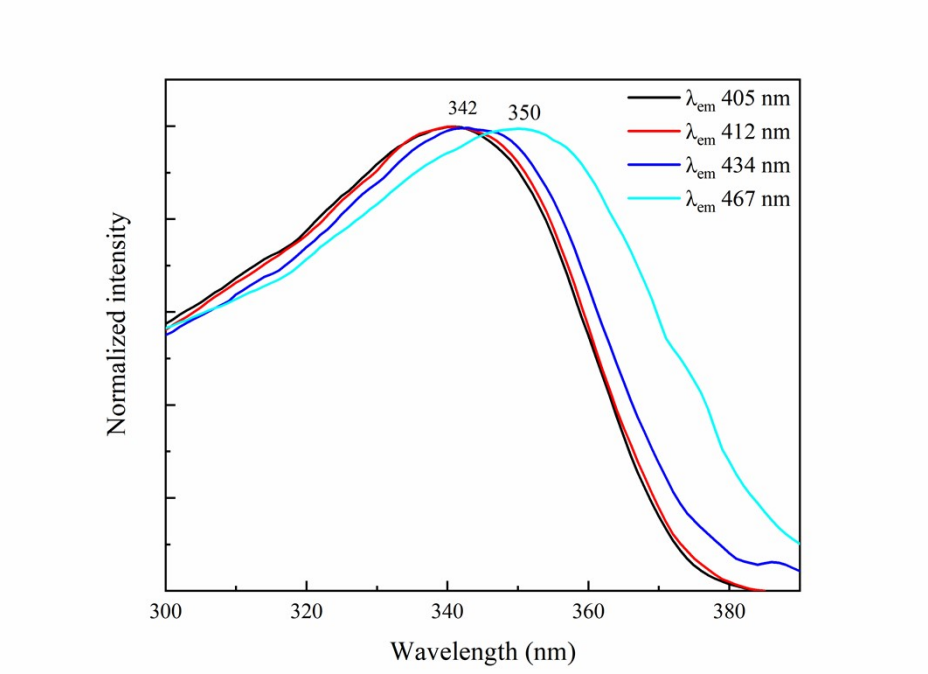

Fig. S15. Excitation spectra of powder **1** at different emission wavelengths

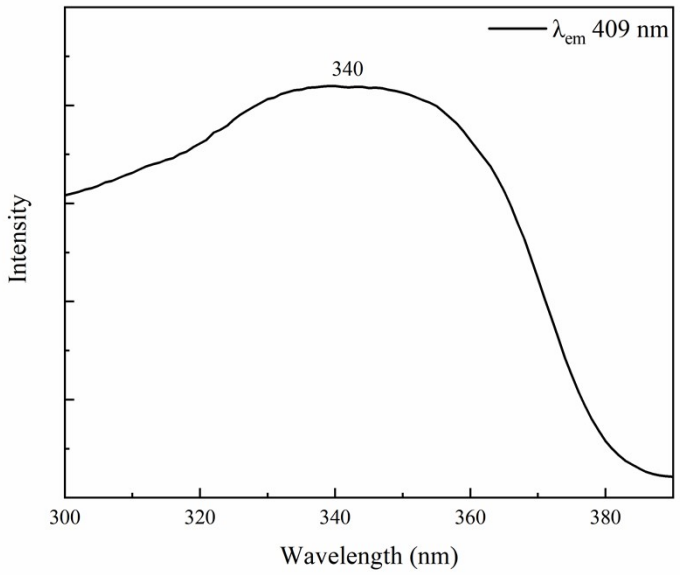

Fig. S16. Excitation spectrum of crystals of **1**

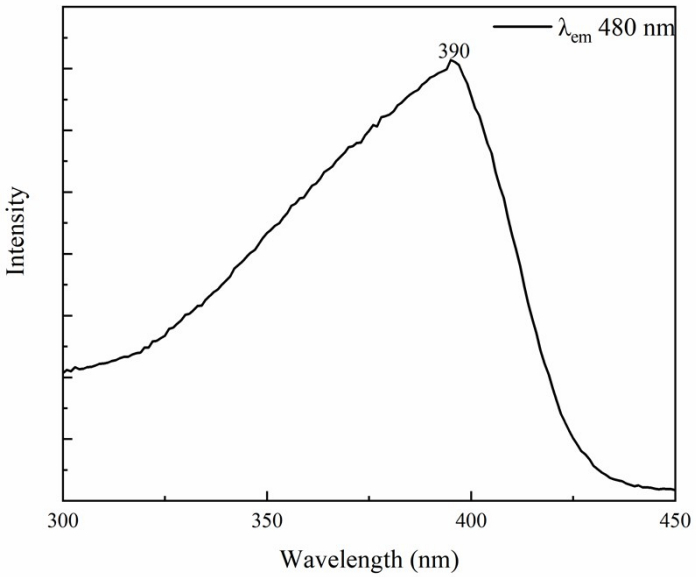

Fig. S17. Excitation spectrum of amorphous **1**

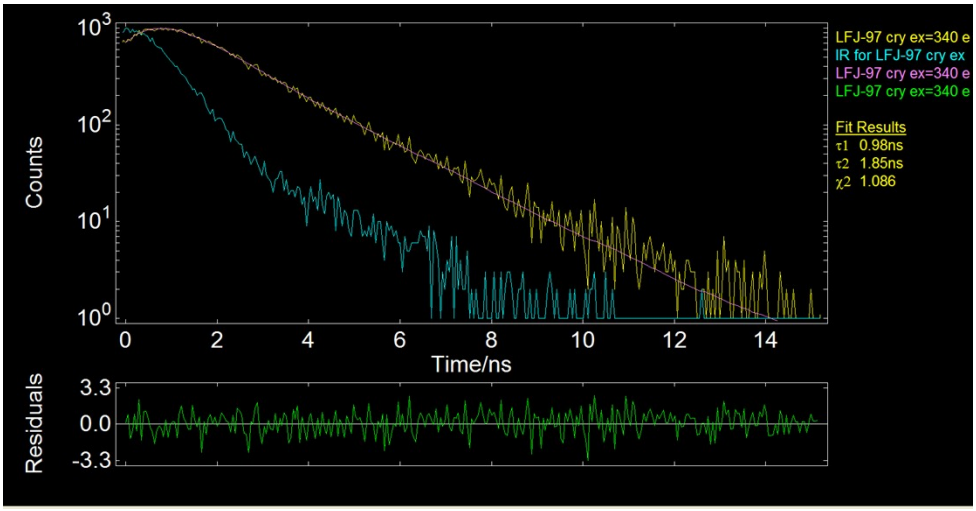

Fig. S18. Fluorescence decay curve of crystals of **1** (λ_{ex} = 340 nm, λ_{em} = 408 nm)

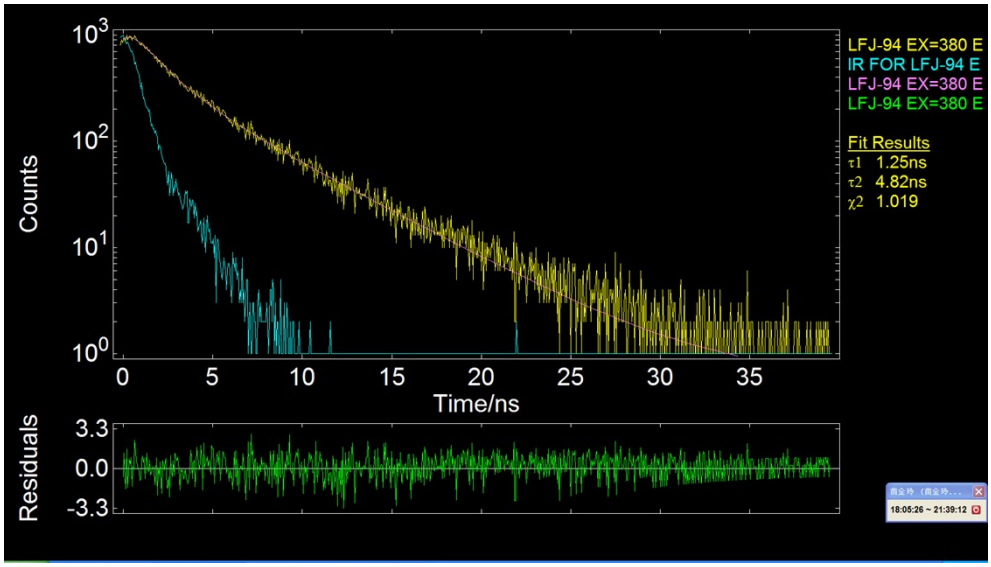

Fig. S19. Fluorescence decay curve of powder of **1** (λ_{ex} = 380 nm, λ_{em} = 467 nm)

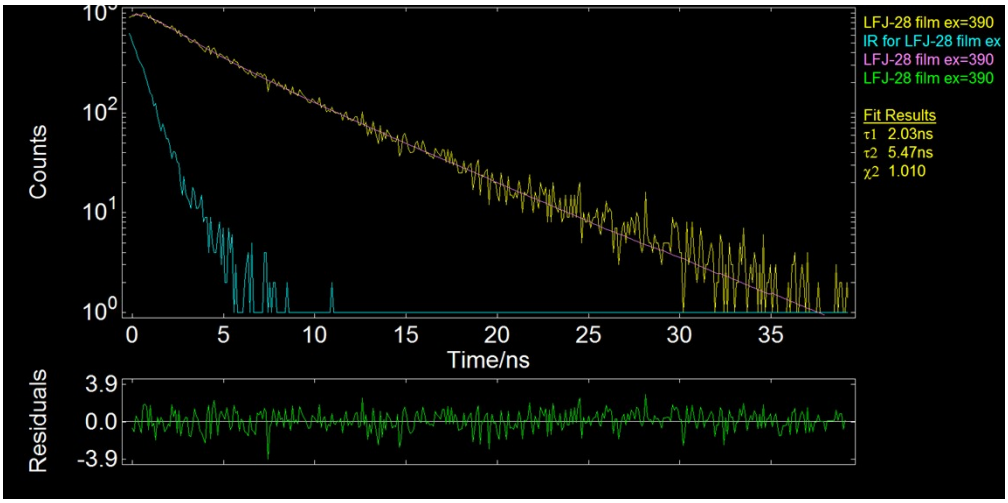

Fig. S20. Fluorescence decay curve of amorphous **1** (λ_{ex} = 390 nm, λ_{em} = 480 nm)

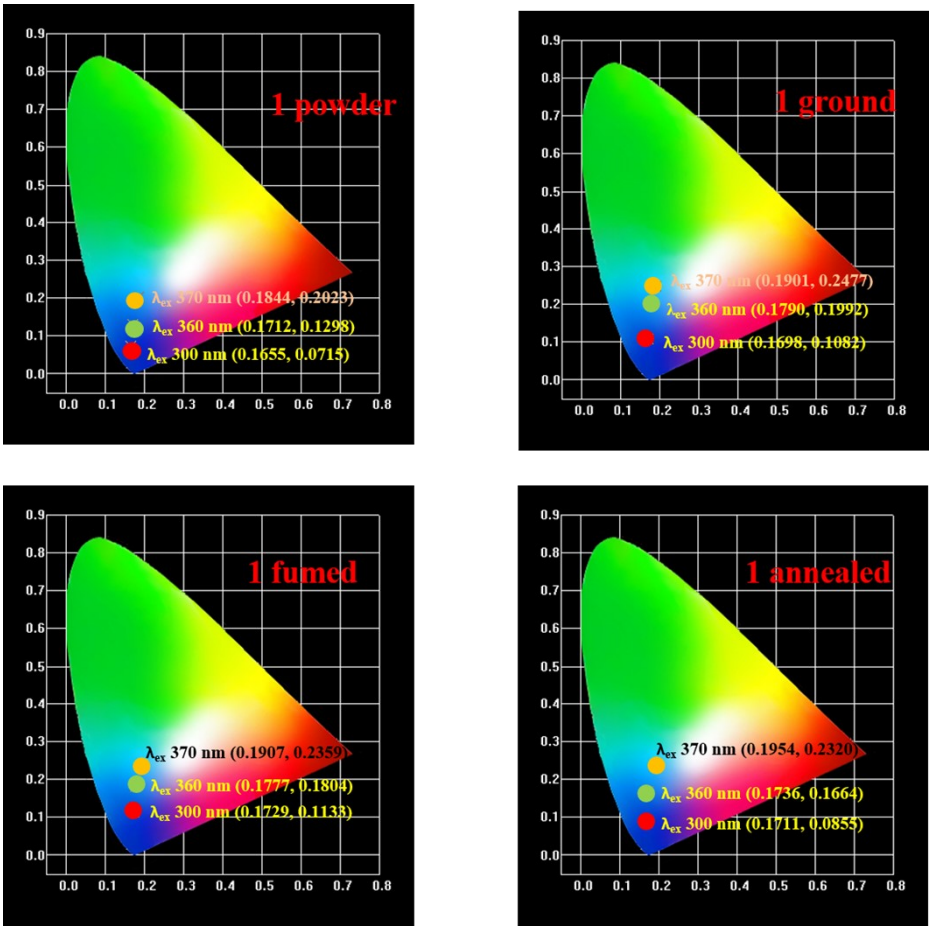

Fig. S21. CIE chromaticity diagrams of **1** (powder), **1** (ground), **1** (fumed) and **1** (annealed)

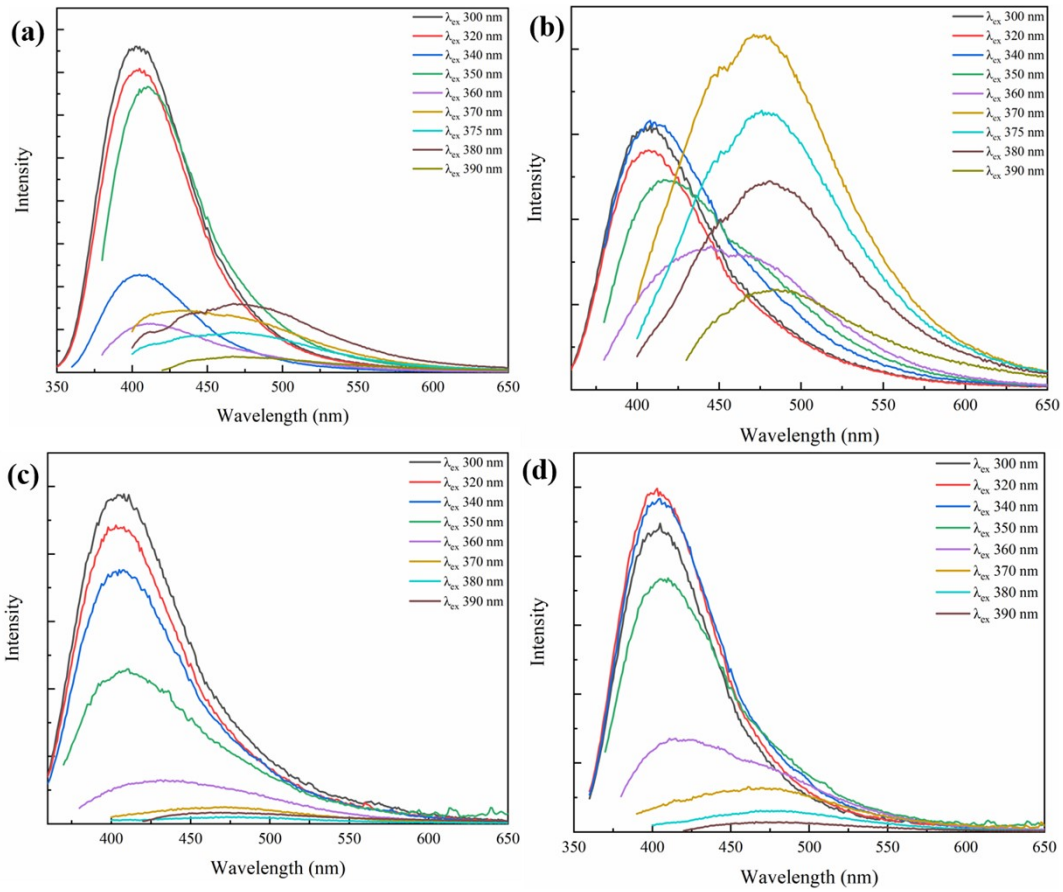

Fig. S22. Emission spectra of compound **1** (a) powder, (b) ground, (c) ground-CH_2Cl_2 fumigation, (d) ground - heated annealing at different excitation wavelengths

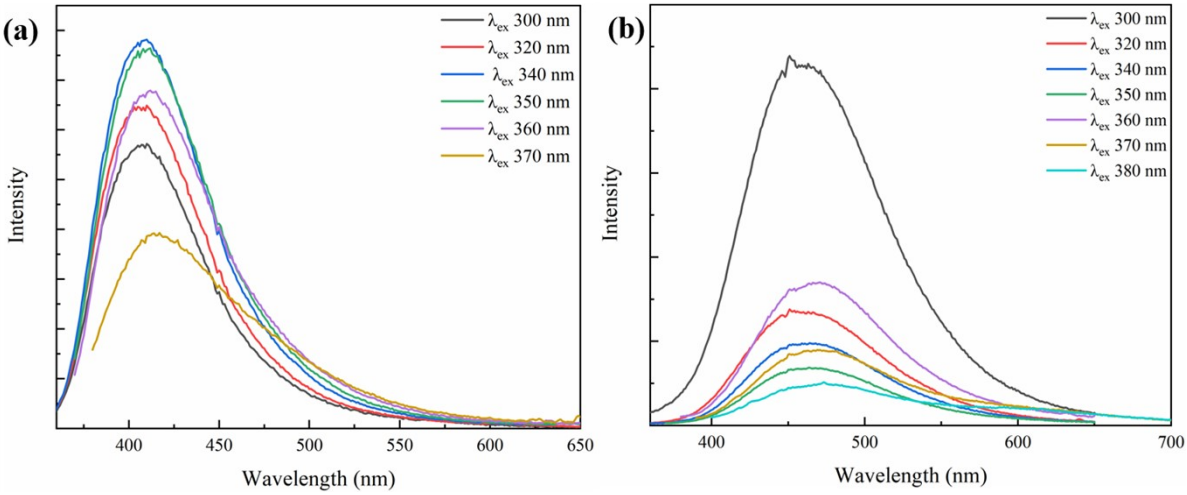

Fig. S23. Emission spectra of compound **1** (a) crystal and (b) amorphous form at different excitation wavelengths

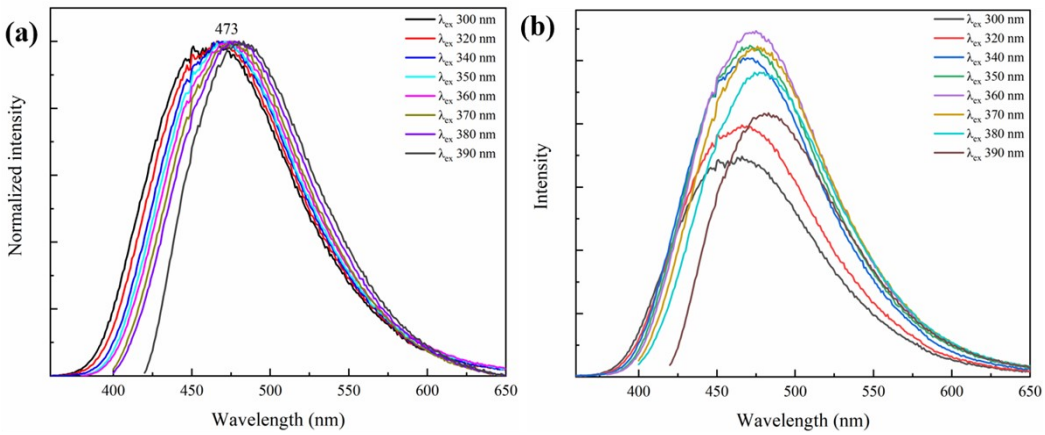

Fig. S24. Emission spectra of compound **2** (ground) at different excitation wavelengths (a: normalized, b: unnormalized)

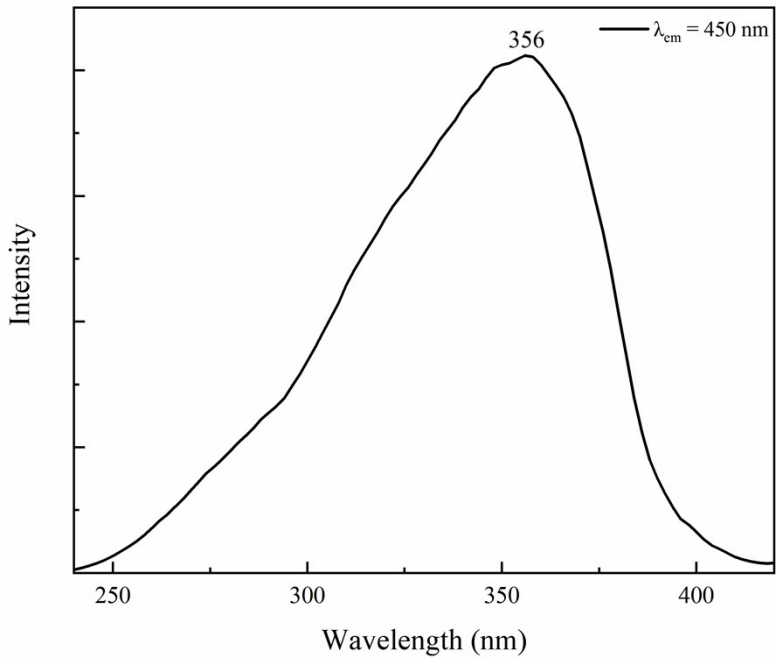

Fig. S25. Excitation spectrum of powder **2**

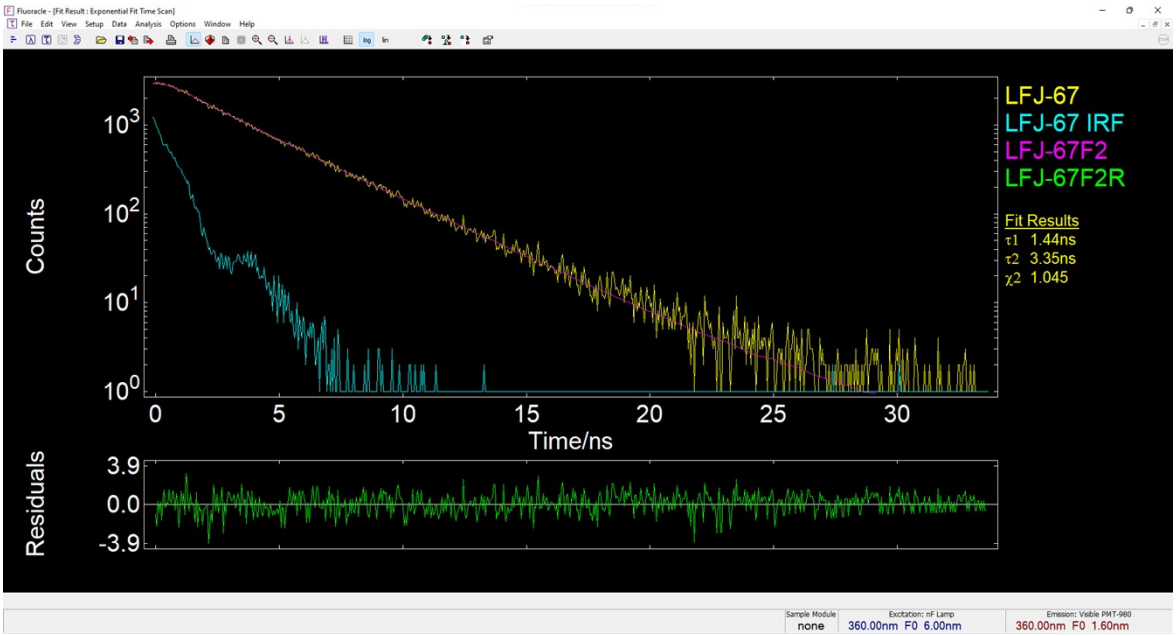

Fig. S26. Fluorescence decay curve of powder **2** (λ_{ex} = 360 nm, λ_{em} = 450 nm)

Table S6 Some photophysical data of compounds **1-2**

	λ_{abs}[a] (nm)	Φ[b]	τ (ns)[b]	k_r[c](s^{-1})	k_{nr}[d](s^{-1})
1	218,308	0.54[e]	3.22	1.68×10^8	1.42×10^8
2	226, 310	0.39[f]	2.96	1.45×10^8	1.93×10^8

[a]Measured in THF, 1×10^{-5}; [b]powder; [c]$k_r = \phi/\tau$; [d]k_{nr} $1/\tau$-k_r; [e]λ_{ex} = 340 nm.